R. & M. No. 3586

R. & M. No. 3586

MINISTRY OF TECHNOLOGY

AERONAUTICAL RESEARCH COUNCIL
REPORTS AND MEMORANDA

A Convergent Nozzle for the Standardisation of Thrust-Rig Measurements

By M. V. Herbert

LONDON: HER MAJESTY'S STATIONERY OFFICE
1969
PRICE 10*s.* 6*d.* NET

A Convergent Nozzle for the Standardisation of Thrust-Rig Measurements

By M. V. Herbert

Reports and Memoranda No. 3586*
July, 1967

Summary.

It is shown that an increase of Mach number from approximately 0·2 to 0·4 at entry to a convergent nozzle of specified shape does not appreciably change its performance. Such a nozzle is thus recommended as a standard device for calibrating the air meter on any thrust rig. For more general application as a means of mass-flow measurement, a value of discharge coefficient can be taken from this work, provided the flow conditions at entry are reasonably uniform, and excluding high temperatures. Use of that value may be subject to certain corrections, and its absolute accuracy when applied to any nozzle of the same nominal specification may not be better than $\pm 0{\cdot}3$ per cent.

CONTENTS

*Replaces N.G.T.E. R.293—A.R.C. 29 991.

CONTENTS—*continued*

LIST OF ILLUSTRATIONS

1. *Introduction.*

During the course of calibrating a new quiescent air thrust rig at N.G.T.E., extensive use was made of several shapes of convergent nozzle, whose performance is given in Reference 1. It was found that certain types of convergent nozzle – namely those with convex curvature and zero wall slope at outlet – can give a very high value of the product 'discharge coefficient × thrust efficiency', and that such a nozzle affords a valuable means of establishing the usually uncertain datum of mass-flow measurement in rigs where an accurate measurement of thrust is available. The rather simple analytical technique involved is given in Reference 1.

In the tests mentioned above, the air was unheated and the Mach number in the parallel approach pipe was low ($\simeq 0{\cdot}2$). Other nozzle test rigs in current use, also operating on unheated air, employ higher entry Mach numbers, thereby representing more closely engine jet-pipe conditions. Having established, for the low entry Mach number of the N.G.T.E. quiescent air rig, the levels of discharge coefficient and thrust efficiency of a particular convergent nozzle shape, recommended as a 'standard' for mass-flow calibration, it is desirable to find whether these levels are more widely applicable. Further tests have therefore been carried out on the same rig, fitted with an arrangement to increase the entry Mach number ($\simeq 0{\cdot}4$).

2. *Nozzle Parameters.*

Convergent nozzle performance may be presented as three quantities† varying with applied pressure ratio:

(i) C_D the discharge coefficient. This rises with increasing pressure ratio until the nozzle is said to be choked, whereafter the flow field in the throat is 'frozen' and C_D constant. By definition, it is always below unity.

(ii) $\eta_{S,\text{conv}}$ the vacuum thrust efficiency. This also becomes constant once the nozzle is choked. It is always above unity by definition.

(iii) $\eta_{F,\text{conv}}$ the gauge thrust efficiency. This rises from a value near unity at pressure ratio around 2 to equal the vacuum thrust efficiency at pressure ratio infinity.

Data in these terms are given in Figure 9 of Reference 1 for the 'standard' convergent nozzle with low entry Mach number. The salient features of those results are

Choking pressure ratio = 2·4

C_D when choked = 0·989

$\eta_{S,\text{conv}}$ when choked = 1·003

} approximately.

3. *Nozzle Approach Geometry.*

The construction, calibration and supposed accuracy of the rig are fully described in Reference 1. The internal shape of the 'standard' convergent nozzle is as given in Figure 8a of that Report, and the present Figure 1 shows it in relation to the approach pipes used for the two series of tests.

It may be noted from Figure 1 that the higher entry Mach number is only achieved a short distance (less than one pipe diameter) ahead of the nozzle contraction. The choice of this arrangement was partly governed by the air-metering system built into this rig, and the manner in which air mass flow is evaluated. Pitot and free-stream static pressures are measured quite a long way upstream of the test nozzle in a pipe of 3·5 in. bore, where the velocity distribution has been carefully examined during initial rig calibration[1]; a further measuring station is provided just ahead of the nozzle, consisting of 4 co-planar wall static tappings. The pressure loss occurring between air meter and nozzle is accounted for by taking the flow function $\frac{Q\sqrt{T_t}}{A P_s}$ derived from the air-meter readings, as explained in Reference 1, and making a correction of the form

$$\left[\frac{Q\sqrt{T_t}}{A P_s}\right]_{\text{entry}} = \left[\frac{Q\sqrt{T_t}}{A P_s}\right]_{\text{meter}} \times \frac{P_{s,\text{meter}}}{P_{s,\text{entry}}} \times \frac{A_{\text{meter}}}{A_{\text{entry}}}.$$

A value of $\frac{A}{A^*}$ corresponding to the entry flow function is then obtained from isentropic-flow tables, which leads to A^* and hence C_D. In applying this relation connecting the two measuring stations, it is necessary to rely on one-dimensional-flow properties. Any considerable change in boundary-layer thickness or velocity profile between the two stations may invalidate this treatment, where accuracy of the order of 0·1 per cent is in question, by introducing uncertainties as to the effective mean total pressure. However, the rig was originally calibrated *via* the thrust performance of convergent nozzles fitted as in the upper part of Figure 1, so that $A_{\text{meter}} \simeq A_{\text{entry}}$, and this arrangement of approach pipe was common to all subsequent nozzles tested on the rig. Thus any defect in the one-dimensional relation above is allowed for by the calibration process, so long as either the approach-pipe geometry remains the same, or the change in velocity profile between measuring stations is not radically altered.

†*See* Notation and Definitions.

At the start of the present exercise, some tests were carried out with a fairly rapid conical contraction from 3·5 in. to 2·5 in. diameter, followed by 13 in. of parallel pipe in which $M_i \simeq 0{\cdot}4$, the position of the wall static tappings relative to the nozzle being similar to the lower part of Figure 1. With that arrangement an apparent increase of 0·3 per cent in C_D was obtained above the value corresponding to the low entry Mach number, and this occurred consistently with 4 of the nozzles used in Reference 1 which had the same circular-arc contraction as the 'standard' nozzle. It was suspected that this effect was associated with boundary-layer growth in the comparatively long length of pipe at the high Mach number.

Accordingly, in the arrangement shown in the lower part of Figure 1, a form of contraction is used which is known[2] to produce uniform axial flow at the station where $dy/dx = 0$, and here the wall tappings are fitted, thus giving the minimum growth of boundary layer ahead of the final measuring station.

In other thrust rigs, in which the air is metered at higher Mach number and close to the nozzle, it may be unnecessary to resort to this geometry of approach pipe; and if a similar choked nozzle is used to calibrate the air meter in that situation, then it may still be quite legitimate to take the nozzle performance as given in this Report. But as a general precaution, when using such a nozzle as a standard device for measurement of air mass flow in different circumstances, it is recommended that the combination of nozzle and approach pipe should follow the principle of Figure 1, in retaining a low Mach number until quite close to the nozzle.

4. *Test Results.*

4.1. *Mass Flow and Internal Pressure Distribution.*

Some re-tests were first made with the original entry arrangement having $M_i = 0{\cdot}19$ (Build A in Figures 1 and 2) in order to check consistency with previous results, and the fresh data (above choking) are shown in Figure 4. This may be compared with Figure 9 of Reference 1, in which the level of C_D is virtually identical†.

For the higher Mach number ($M_i = 0{\cdot}41$) it was first decided to use the same nozzle unit, with a fillet inserted to match the new approach pipe (B in Figure 1). This arrangement is shown in Figure 2, and is referred to as Build B1. The fillet was made of araldite, moulded to the nozzle surface and the bore machined. Tests with this build produced the data for C_D appearing in Figure 5. The level is the same to within 0·1 per cent as in Figure 4.

Mach numbers at the nozzle wall along the contraction region, obtained from 7 wall static-pressure tappings indicated in Figure 1, are compared in Figures 6 and 7. While substantial differences exist some way ahead of the throat, as might be expected with a sharp corner for the flow to negotiate, the values reached at the last tapping (0·02 throat diameters from outlet) agree quite closely: $M = 1{\cdot}214$ for Build A and 1·204 for Build B1. Figure 7 further shows that this wall Mach number levels off at the same value of pressure ratio in each case.

One may note that, to the accuracy to which C_D is capable of being determined, that curve is level above pressure ratio 2·4 (Figure 5), the choking value quoted earlier, whereas the final wall Mach number in Figure 7 is still increasing slightly up to pressure ratio 3. However, such small changes in Mach number would produce a scarcely detectable effect on C_D, and since the latter quantity is generally of more interest, it seems preferable to continue referring to the nozzle as choked at the lower pressure ratio.

In sum this evidence implies that, so far as mass flow is concerned, the nozzle performance has not been altered appreciably by the change of entry Mach number. The very small differences observed in C_D

†It may be noted that the scatter in C_D between different runs in Figures 4, 5 and 14 of the present Report is somewhat less than that generally shown in Reference 1. This slight improvement stems from correction of an error in the original treatment of mass flow (Section 3.1 of Reference 1). The value of air meter 'form factor', defined as the ratio of average to centreline P_t, was obtained from a particular set of traverses, and thereafter regarded as constant for a given nozzle throat area. In fact, slight variation should be introduced with alteration of C_D, which tends to compensate for that alteration. This it is now the practice to include.

($< 0{\cdot}1$ per cent) and final wall Mach number (0·01) are mutually consistent, and suggest a slight increase in the effective curvature of the displacement boundary[1] at outlet when $M_i \simeq 0{\cdot}4$. But the effect is hardly significant within ordinary standards of measurement.

4.2. *External Pressure Distribution.*

It would thus be expected that the thrust efficiency given by the nozzle must also remain similar. But direct measurement of thrust according to the system described in Reference 1 showed that the efficiency of Build B1 apparently fell about $\frac{1}{2}$ per cent lower at pressure ratios in the range 2 to 5. This discrepancy implied the neglect of some extra force in the thrust balance, and led to detailed investigation of the pressure distribution around the outside of the nozzle in both Builds A and B1.

In the early stages of rig development, some work was done to ensure a negligible differential pressure acting on the large area of nozzle flange close to its outlet plane – *see* Figure 2. From this grew the standard practice of fitting a baffle plate around the nozzle base as illustrated in Figure 3, the annular clearance being typically about $\frac{1}{8}$ inch. It is also customary to instrument the base itself, usually $\frac{1}{8}$ inch or less in width, with 6 pressure tappings, and the force thus derived is included in the thrust balance. Near the design-point of any nozzle, the circumferential distribution of base pressure tends to be uniform; elsewhere it can vary in a random manner.

For the present purpose 10 additional pressure tappings were fitted outside the base in the rearward-facing surface of the nozzle of Builds A and B1. In both cases it was found that the general magnitude of pressure differences in relation to the reference pressure P_c (Figure 3) increased with A.P.R.; subsequent tests, using isolated pressure probes attached to the upstream and downstream faces of all pipe flanges within the depression box, showed that a similar increase in differential pressure occurred uniformly on all surfaces, which therefore balanced each other. The actual values of external pressure difference involved were equivalent to less than 1 inch of water throughout, but acting on a large total projected area.

With Build A ($M_i \simeq 0{\cdot}2$), at low values of A.P.R. around the condition taken for the original analysis of losses and rig calibration described in Reference 1, the differential pressures on the rearward-facing surface of the nozzle were very small and had a randomly-distributed variation in sense, so that the net extra force was confirmed as negligible. With Build B1 ($M_i \simeq 0{\cdot}4$) at low A.P.R., however, these pressure differences were rather greater, while their sense was now constant (a suction) and the net force no longer negligible, being in the direction required to augment thrust.

Other quite considerable disparities between the two builds were observed. Figure 8 shows that the mean base pressure difference is generally negative with $M_i \simeq 0{\cdot}2$. At pressure ratios below the region of instability, the pressure difference is quite uniform circumferentially around the base (Figure 9a)†, and again at the highest A.P.R., but in between it assumes a distorted pattern – in some places negative and in some positive, but with diametral symmetry (Figure 9b). In contrast, the mean base pressure difference with $M_i \simeq 0{\cdot}4$, given in Figure 10, is positive at all pressure ratios below 7. The circumferential distribution of base pressure difference is no longer either uniform or symmetrical in most cases (Figures 11a and b).

In comparing Figures 9 and 11, it may be noted that the base pressure tappings numbered 1 to 6 were identical between the two runs, and the connections undisturbed. The baffle plate, however, may not have been in exactly the same location relative to the nozzle. Successive assemblies of nominally the same build have given values of mean base pressure difference which do not very closely repeat the data of Figures 8 and 10, even allowing for a limit of 0·1 inch of water reading accuracy (*see* Figure 8). Such variations can only be attributed to minor changes in baffle-plate location. With another baffle plate of dished shape on one build, both base and external pressure differences were considerably altered.

It is of some interest to note more particularly the relation between mean base pressure (P_b) and the reading of the nearest pressure tapping on the external boat-tail surface ($P_{ext,1}$). With $M_i \simeq 0{\cdot}2$, we have seen that $P_b > P_c$, while in most cases $P_{ext,1} < P_c$, this opposition of signs applying generally at all pressure ratios, but without any consistency of relative magnitudes. With $M_i \simeq 0{\cdot}4$, $P_{ext,1} < P_c$ throughout; at low pressure ratio $P_b < P_c$ also, the signs being thus the same, and the relative magnitudes are similar;

†A perfectly uniform distribution would appear in Figures 9 and 11 as a regular hexagon.

but at high pressure ratio when $P_b > P_c$ the signs are opposite once more. Hence one can sum up by saying that the behaviour of the two builds has common features at high A.P.R., but fairly radical differences at low values near the design-point.

This investigation into external pressure distributions has shown that a baffle plate as customarily fitted is not always adequate to eliminate forces on closely-adjacent flanges. In order to obtain a correct measurement of thrust with Build B1, a very comprehensive system of pressure instrumentation would be required, considering the probability of circumferential non-uniformity of external pressures. Accordingly a fresh nozzle was made for $M_i \simeq 0{\cdot}4$, integral with the contraction section of the approach pipe, thus removing the flange well upstream and creating minimum boat-tail. This is called Build B2, and is illustrated in Figure 2.

Two alternative baffle plates were used in conjunction with this new nozzle, located as shown in Figure 3, one at outlet as with all previous builds, and the other on the parallel portion of afterbody. It will be seen from Figures 12 and 13 that the variation of mean base pressure difference with A.P.R. is quite dissimilar in the two arrangements, and in neither case resembles at all closely that for Build B1 (Figure 10). One common feature amongst all builds with $M_i \simeq 0{\cdot}4$ is that this pressure difference changes from negative at high A.P.R. to positive at low, unlike that with $M_i \simeq 0{\cdot}2$.

Comparison of Figures 8, 10, 12 and 13 shows that all builds, regardless of the value of M_i, produced a region of instability somewhere between A.P.R. 3 and 5; this was accompanied by a large change in the level of base and boat-tail pressure differences, and a clearly distinguishable whistling tone emitted by the rig. Accurate thrust measurement in the unstable region was virtually impossible. Another phenomenon encountered on all builds was a violent 'hammering' noise somewhere in the range of A.P.R. 11 to 13, caused by rapid and easily visible vibration of the baffle plate. This effect occurred between two regimes of widely different base-pressure level (e.g. Figure 12), and there was evidence of some hysteresis, the A.P.R. being slightly higher when approached from below than when from above.

One may note that both the phenomena just described occurred at values of A.P.R. associated more closely with baffle-plate position than with change of M_i–with the baffle plate in the nozzle outlet plane (which was approximately the same distance from the end of the depression box in every case), all builds exhibited instability around A.P.R. $4\frac{1}{2}$, while movement of the baffle plate on Build B2 altered this to $3\frac{1}{2}$; similarly, the baffle plate vibrated at A.P.R. $11\frac{1}{2}$ when at outlet, but at 13 when moved to the parallel portion of Build B2. It is not possible to say whether the critical factor is the distance between baffle plate and nozzle outlet or that between baffle plate and diffuser, but it seems fairly clear that both the instability and the baffle-plate vibration are essentially 'external' effects, and probably associated with the particular geometry of depression box and diffuser in this rig.

4.3. *Thrust.*

Thrust data obtained with Build B1 were discarded for the reason mentioned in Section 4.2. The final arrangement used was Build B2 with baffle plate on the parallel portion of afterbody (*see* Figure 3), and 4 pressure tappings on the conical boat-tail downstream. It was confirmed that the differential pressures were the same on both forward and rearward-facing surfaces everywhere upstream of the baffle plate, the magnitude of this pressure difference altering with A.P.R. as previously described.

While values of C_D from Builds A and B1 are directly comparable, being physically the same piece of metal at the throat, those from the new nozzle of Build B2 are not. The latter was manufactured to the same nominal profile, but earlier work[1] has shown that on this small scale of model variations of $\pm 0{\cdot}2$ per cent in mean C_D are still possible. In fact the curve of C_D for Build B2 (Figure 14) levels off at 0·988, as compared with 0·990 for B1 (Figure 5), the choking pressure ratio being around 2·4 in each case. Such differences in C_D should, however, have negligible effect on thrust efficiency.

It may be mentioned in passing that, during the course of the present work, wet air was used for some tests and dry air for others with the same build. In line with previous experience of convergent nozzles, no effect could be detected on C_D, mean base pressure difference or thrust efficiency.

The values of thrust efficiency for Build B2 given in Figure 14 include the boat-tail force; however, this amounted to less than 0·1 per cent throughout. When comparing Figures 4 and 14, it must be borne in mind that the magnitude of any corresponding external force correction for Build A is somewhat

uncertain, due to inadequate coverage of instrumentation, but existing data suggest that such a correction is probably limited to around 0·1 per cent.

Below choking pressure ratio the curve of vacuum thrust efficiency ($\eta_{S,\text{conv}}$) in Figure 14 turns upwards slightly to match the downwards turn of C_D, as is normal behaviour. Above choking a mean value of $\eta_{S,\text{conv}}$ in both Figures 4 and 14 is about 1·002, smoothed curves varying from that value within $\pm 0{\cdot}001$. There does not therefore seem to be any significant difference in thrust performance with change of M_i.

4.4. *Recommendations.*

So far as the use of a convergent nozzle for thrust-rig calibration is concerned, the first and most obvious point to emerge from this exercise is the inadvisability of having a large flange or other rearward-facing surface in close proximity to the nozzle outlet. It would be preferable to have the nozzle mounted on a sleeve or screwed fitting, and if some flange is unavoidable then it should be placed as far away from the nozzle outlet as possible. Whatever boat-tail remains should contain pressure tappings, and the resulting force, as well as that on the base if any, should be included in the measured thrust.

Secondly, the calibration should extend to as high an A.P.R. as possible, the preferred range being 6 and upwards. At low A.P.R., and especially in the vicinity of choking, external conditions are much more unsteady (at least on this rig), and result in considerably wider scatter of thrust data – *see* Figures 4 and 14, also Figures 9 to 11 of Reference 1.

5. *General Application.*

The tests described in Sections 3 and 4 justify the conclusion that changes of entry Mach number up to 0·4 do not appreciably affect the performance of a convergent nozzle with this shape. Such a nozzle is therefore potentially useful as a 'standard' for comparing the accuracy of existing thrust rigs and for calibrating the air-metering system on new ones. The actual performance levels quoted here, however, relate to the conditions of this particular rig, and may not necessarily apply under all circumstances. It is worth examining in turn some of the effects which might modify them.

5.1. *Effect of Reynolds Number.*

A question which not infrequently arises when considering any device for airflow calibration is that of how its C_D may be expected to vary with Reynolds number. Component flow defects of the nozzle shape of Figure 1 above choking are discussed in detail in Reference 1, and it is shown that with a C_D of 0·989 the losses at the condition of this rig may be divided approximately into 0·003 from friction and 0·008 from curvature. The former figure was taken from Reference 3 for $Re^* = 0{\cdot}75$ million, at which value it is independent of whether the boundary layer be turbulent or laminar. According to Figure 8 of Reference 3, the extreme variation of this flow defect over the range $10^5 < Re^* < 10^7$, making suitable assumptions regarding boundary-layer state, could change it by a factor of 2 either way – that is to say it could vary between 0·0015 and 0·006, giving a variation of C_D between 0·9905 and 0·986 if the curvature component remained unchanged. However, it was further shown in Reference 1 that the effective curvature of this nozzle is apparently reduced by the existence of a boundary layer, the theoretical inviscid-flow defect from curvature being perhaps 0·018. If this is the case, there should be some mutual compensation between the effects of friction and curvature which would tend to restrain the variation of C_D within closer limits than those just postulated. Unfortunately, no sufficiently accurate test data are at present available for the nozzle at other levels of Re^*, so that any correction must be a matter of some uncertainty.

With regard to thrust, the analysis of Reference 1 shows that either form of thrust efficiency departs from unity to an extent less than does C_D. An average value of this factor is probably around 0·3 to 0·4, depending on Reynolds number, boundary-layer state, and the treatment of curvature†. It therefore seems probable that the variation of $\eta_{S,\text{conv}}$ corresponding to the above change of C_D would at most only be from 1·0025 to 1·004.

It should be noted that the assumption of corrections as above has a not insignificant effect upon the product $C_D \cdot \eta_{S,\text{conv}}$, which would move by up to 0·3 per cent over that range of Re^*. This product, as was pointed out in Reference 1, is independent of mass-flow measurement, and is proportional to the actual thrust force produced by the nozzle. When calibrating a thrust rig, this measured force is the one quantity which should be known *a priori* to quite high accuracy, and thus the rig will be able to provide a numerical value of $C_D \cdot \eta_{S,\text{conv}}$ for its particular operating conditions. The breakdown of this product then becomes a matter for analysis after the manner of Reference 1, or of assumption based on some independent arbiter of mass-flow estimation.

It would no doubt be possible to construct one or more thrust rigs to operate at different levels of Re^*, and by examining the variation of $C_D \cdot \eta_{S,\text{conv}}$ to try and check on the validity of the above corrections. But in practice a thrust rig for nozzle testing will ordinarily be required to operate at a level of Re^* fairly representative of full-scale engine conditions, which would be in the region of 4 to 10 million. In that range the effect of Reynolds number on the product $C_D \cdot \eta_{S,\text{conv}}$ could amount at the most to a difference of 0·1 per cent from its value at the conditions applying in Reference 1 and the present work. Even the possible difference in C_D is then only 0·15 per cent, which is pretty well on the limit of accuracy which can be hoped for with ordinary means of measurement. For the purposes of thrust-rig calibration, therefore, it is thought that the Reynolds number effect on performance of a standard nozzle can probably be neglected.

5.2. *Real-air Effect.*

The nozzle entry stagnation conditions in Reference 1 and the present tests were approximately 1 atm and 290°K. Isentropic quantities have been derived on the assumption of constant $\gamma = 1{\cdot}400$. A very careful and comprehensive treatment by Ascough[5] has shown that the resultant error is negligible at these conditions. However, the error involved in taking this value for γ would become considerably greater with either increase in pressure or decrease in temperature; at 10 atm and 290°K, for instance, it would amount to an over-estimate of 0·4 per cent in C_D and an under-estimate of about 0·4 per cent in thrust efficiency. The product $C_D \cdot \eta_{S,\text{conv}}$ would thus remain approximately correct. But unless appropriate alteration were made to the isentropic quantities, any breakdown of the product would be seriously in error.

The values of C_D and thrust efficiency of a convergent nozzle, based on isentropic flow of the *real* fluid, should be constant regardless of pressure and temperature (at least up to 500°K, and assuming homogeneity of flow). Supposing that a standard convergent nozzle is used to calibrate the air meter of a thrust rig, and that the measured force yields the familiar product value of approximately 0·992 above choking, then, using the notation of Reference 5, $C_{D,\text{real}}$ should be taken as around 0·989. The apparent value of C_D corresponding to $\gamma = 1{\cdot}400$ ($= C_{D,\text{classic}}$) will be higher by the factor

$$\frac{C_{D,\text{classic}}}{C_{D,\text{real}}} = \frac{(\rho V)^*_{\text{real}}}{(\rho V)^*_{\text{classic}}} \text{ given in Reference 5.}$$

†In Reference 1 a curvature factor is defined as

$$\lambda = \frac{\eta_{S,\text{conv,c}} - 1}{1 - C_{D,\text{c}}}$$

where suffix c refers to the component due to curvature alone. On the evidence of a convergent nozzle tested in Reference 4, with 40° half-angle conical contraction, in which the friction component is insignificant in comparison to that from curvature, a reasonable estimate for λ should be close to 0·3.

If the rig were operating at the conditions of the example above, then $C_{D,\text{classic}}$ would be about 0·993. Corresponding values of efficiency, which we will call $\eta_{S,\text{conv,real}}$ and $\eta_{S,\text{conv,classic}}$, would then be around 1·003 and 0·999 respectively. The latter value, it may be noted, is below the theoretical lower limit of unity, which only reflects the artificial situation associated with the use of isentropic quantities derived on the basis of $\gamma = 1{\cdot}400$.

5.3. *Manufacturing Tolerance.*

It was mentioned in Reference 1 that tests on this rig of a family of 7 convergent-divergent nozzles, all having their contraction nominally identical with the standard convergent nozzle (Build A), disclosed a total variation of 0·4 per cent in mean C_D (0·9875 to 0·9915), each nozzle being itself consistent within a scatter band of about $\pm 0{\cdot}1$ per cent. This situation could only be attributed to minor inexactitudes of machining, resulting in local differences of effective curvature in the immediate vicinity of the throat. On the scale of these models, with 2·0 inch throat diameter, errors of less than 0·001 inch in wall profile would be required to account for such changes in the flow defect due to curvature. Increase of model scale in other applications should reduce the uncertainty from this cause.

The mean C_D value of 0·989 obtained for the standard convergent nozzle is in fact near the middle of the range of variation quoted above, which inspires some confidence in accepting it as genuinely applicable to the design of contraction shown in Figure 1. However, the certainty of determining mass flow in general on this rig is not claimed to be better than $\pm 0{\cdot}2$ per cent[1]. Thus if a new nozzle is made to the same nominal specification as in Figure 1, for use as a standard of airflow measurement elsewhere, the assumption of a value for its mean C_D (i.e. ignoring point-to-point scatter) must take account of two factors. The first is the uncertainty of rig datum which attaches to all the results given herein ($\pm 0{\cdot}2$ per cent); and the second is the uncertainty from manufacturing accuracy (less or possibly more than $\pm 0{\cdot}2$ per cent depending on scale). Putting these together on a root-sum-of-squares basis, one arrives at an overall uncertainty of around $\pm 0{\cdot}3$ per cent, and the absolute value of mean C_D for such a nozzle cannot be guaranteed by the present work to better than this amount.

5.4. *Entry Flow Conditions.*

The rig used for these tests operates with unheated air delivered down a smooth parallel pipe at comparatively low Mach number. Both total temperature and static pressure are known to be uniform ahead of the final contraction, and the flow is free from serious pulsations. Calculations of boundary-layer thickness and total pressure measurements made during development of the rig both suggest that fully-developed pipe flow is not achieved at the end of the parallel pipe.

As already stated, the performance of the standard nozzle given here is only appropriate to the rig conditions just enumerated; in different circumstances the same nozzle could very well change its flow and thrust characteristics, but any quantitative estimate of particular effects is at present impossible. It is thought that any choked nozzle with rapid contraction to the throat would be relatively insensitive to either moderate pulsations or moderate profile distortions in the approach flow. Severe static-pressure gradients, however, such as might be produced by a bend just ahead of the nozzle, or major variations of temperature, as could occur with hot gas flowing between cooled walls, are certainly outside the range of application which the present data may be expected to have.

If a thrust rig is to be calibrated which inescapably includes such serious departures from previous practice, then it is still recommended that a nozzle of standard convergent shape be used, but breakdown of the product $C_D.\eta_{S,\text{conv}}$ must be carried out from first principles, using some method of analysis equivalent to that in Reference 1. In circumstances where only mass-flow measurement is of interest, such abnormal flow conditions should not be encountered; if they cannot be avoided, the consequent uncertainty must be accepted or some other form of flowmeter introduced.

6. *Conclusion.*

It is shown that an increase of Mach number from approximately 0·2 to 0·4 at entry to a convergent nozzle of specified shape does not appreciably change its performance. Such a nozzle is thus recommended as a standard device for calibrating the air meter on any thrust rig. For more general application as a means of mass-flow measurement, a value of discharge coefficient can be taken from this work, provided the flow conditions at entry are reasonably uniform, and excluding high temperatures. Use of that value may be subject to certain corrections, and its absolute accuracy when applied to any nozzle of the same nominal specification may not be better than ± 0·3 per cent.

Acknowledgement.

The author wishes to thank Dr. B. S. Stratford for helpful discussion of early results.

NOTATION AND DEFINITIONS

A.P.R. Applied pressure ratio

$$= \frac{\text{nozzle entry total pressure}}{\text{base pressure}}$$

C_D Discharge coefficient

$$= \frac{\text{measured air mass flow}}{\text{isentropic air mass flow for the same throat area at the same total pressure and total temperature}} = \frac{A^*}{A_q}$$

$\eta_{F,\text{conv}}$ Gauge thrust efficiency

$$= \frac{\text{gauge thrust of actual convergent nozzle}}{\text{gauge thrust of an isentropic convergent nozzle, passing the same flow, at the same A.P.R.}}$$

$\eta_{S,\text{conv}}$ Vacuum thrust efficiency

$$= \frac{\text{vacuum thrust of actual convergent nozzle}}{\text{vacuum thrust of an isentropic convergent nozzle, passing the same flow}}$$

Re^* Nozzle throat Reynolds number, based upon sonic flow conditions and the diameter of a circle having the same area as the nozzle throat

A^* Throat area of isentropic nozzle required to pass actual mass flow

A_q Throat area of actual nozzle

M Mach number

P Pressure

Q Mass flow

T Temperature

Suffices

b Base

c Depression box (*see* Figure 3)

i In nozzle approach pipe

s Static

t Total head

REFERENCES

No.	*Author(s)*	*Title, etc.*
1	M. V. Herbert, D. L. Martlew and R. A. Pinker	The design-point performance of model internal-expansion propelling nozzles with area ratios up to 4. A.R.C. R. & M. 3477. December 1963.
2	J. C. Ascough	The development of a nozzle for absolute airflow measurement by pitot-static traverse. A.R.C. R. & M. 3384, 1963, and subsequent unpublished work in Ministry of Aviation.
3	B. S. Stratford	The calculation of the discharge coefficient of profiled choked nozzles and the optimum profile for absolute mass flow measurement. J. R. Aero. Soc., Vol. 68, No. 640. April 1964 (originally issued by M.O.A., June 1962).
4	M. V. Herbert, J. S. Drabble and G. T. Golesworthy	Model tests of a two-stream nozzle with divergent shroud. M.O.A. internal paper, December 1965.
5	J. C. Ascough	Real-air effects in propelling nozzles. A.R.C. R. & M. 3522. September 1966.

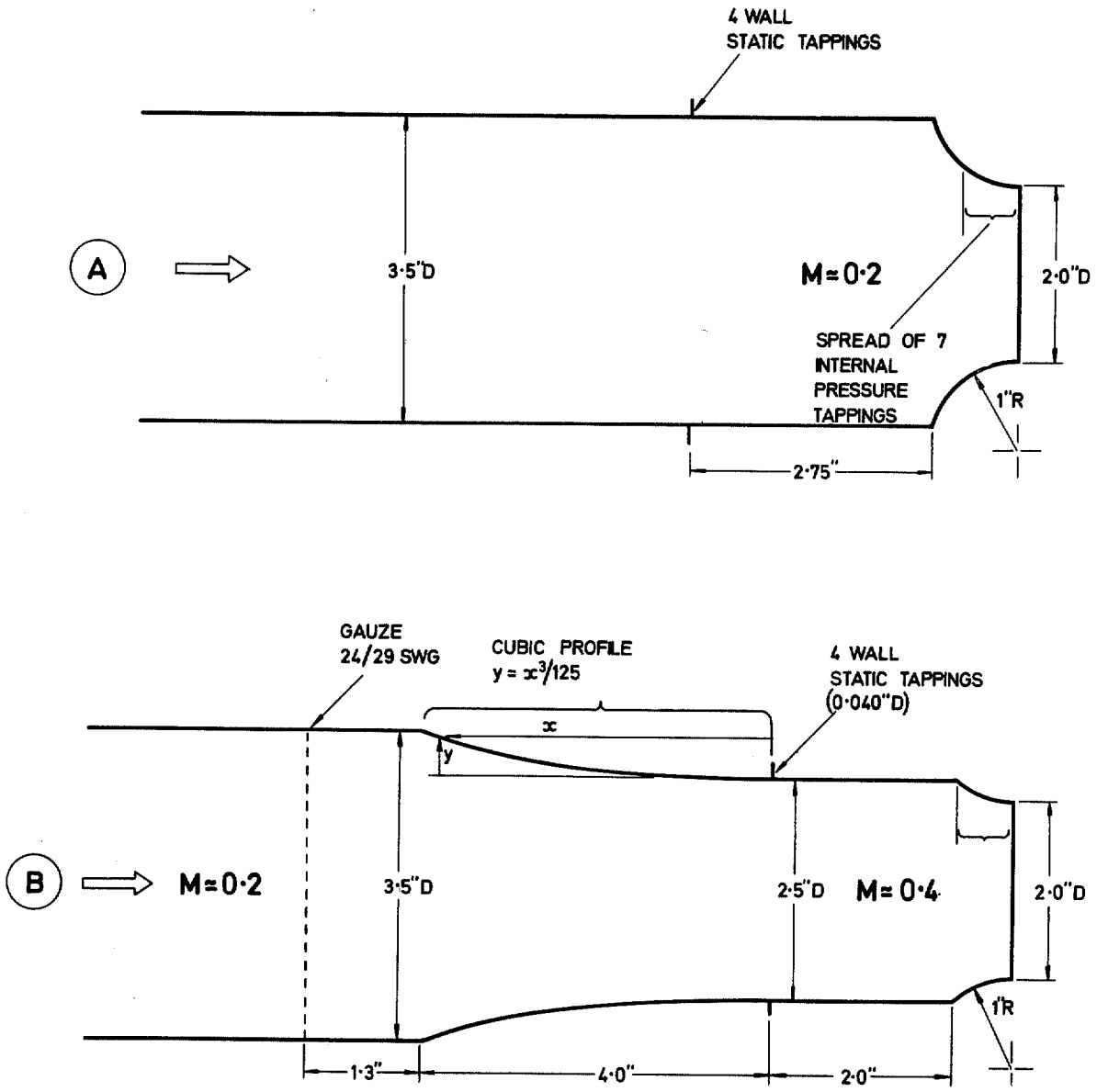

FIG. 1. Internal arrangements of nozzle and approach pipe.

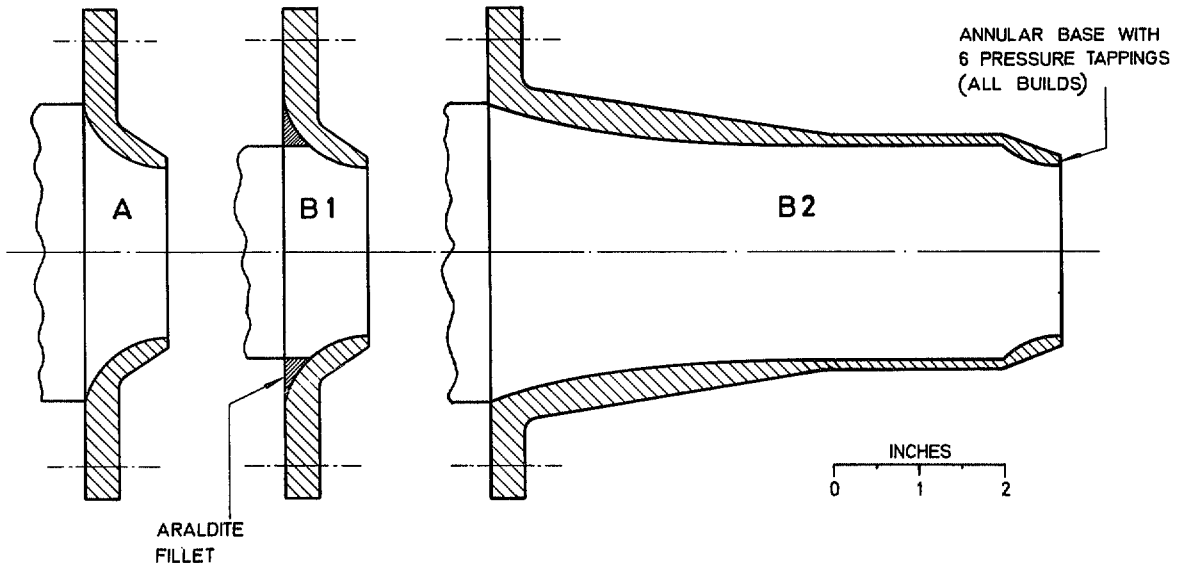

FIG. 2. External geometries of nozzle.

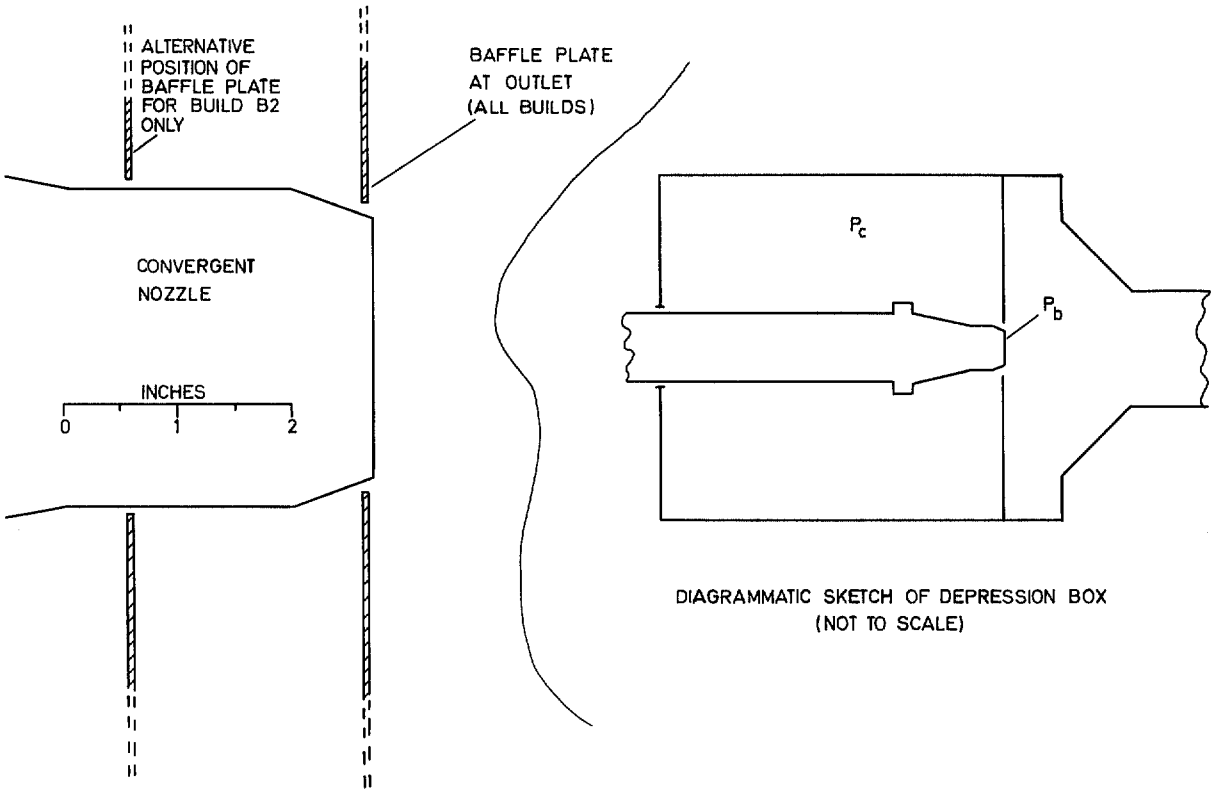

FIG. 3. Position of baffle plate in quiescent air rig.

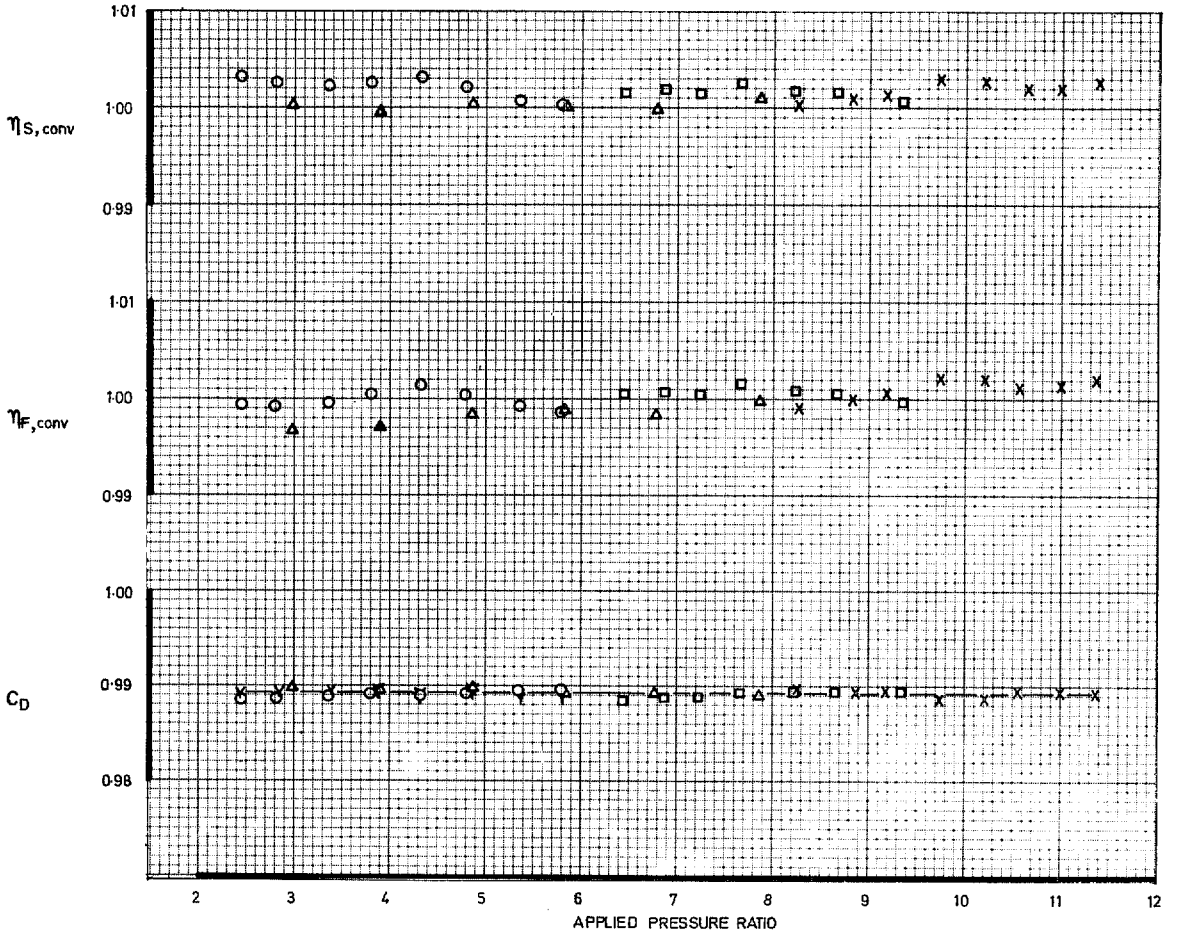

FIG. 4. Performance of nozzle with $M_i \simeq 0{\cdot}2$ (Build A).

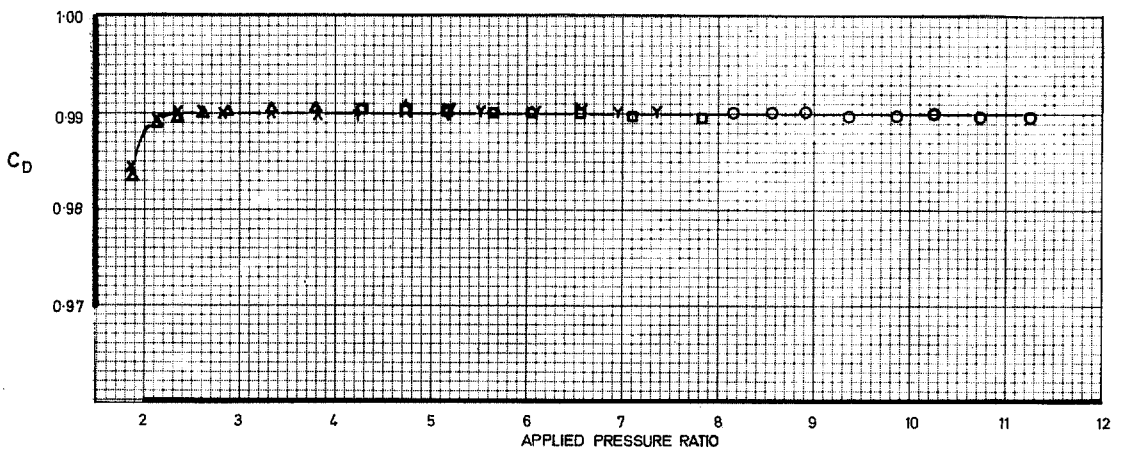

FIG. 5. Discharge coefficient of nozzle with $M_i \simeq 0{\cdot}4$ (Build B1).

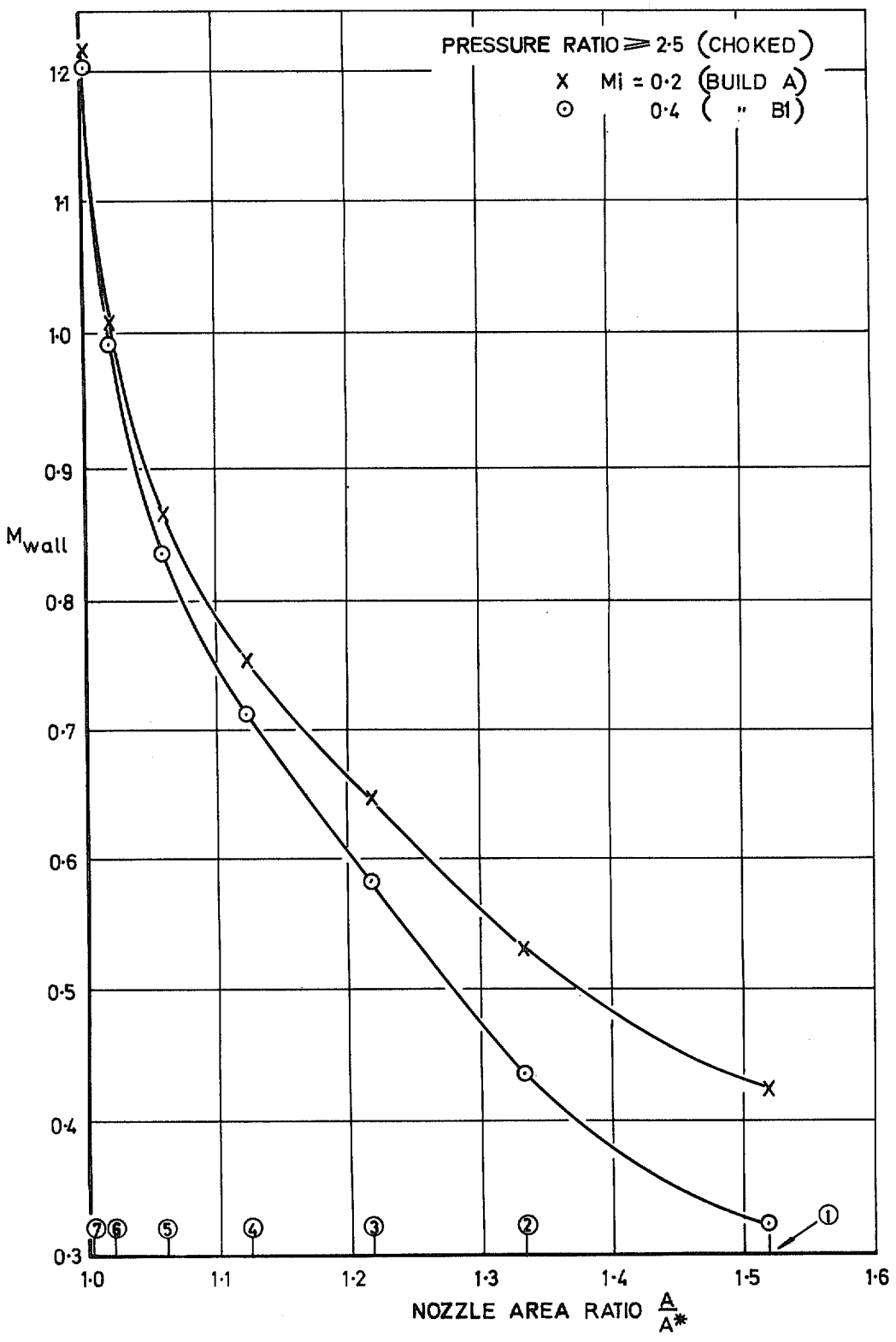

FIG. 6. Internal conditions at nozzle wall.

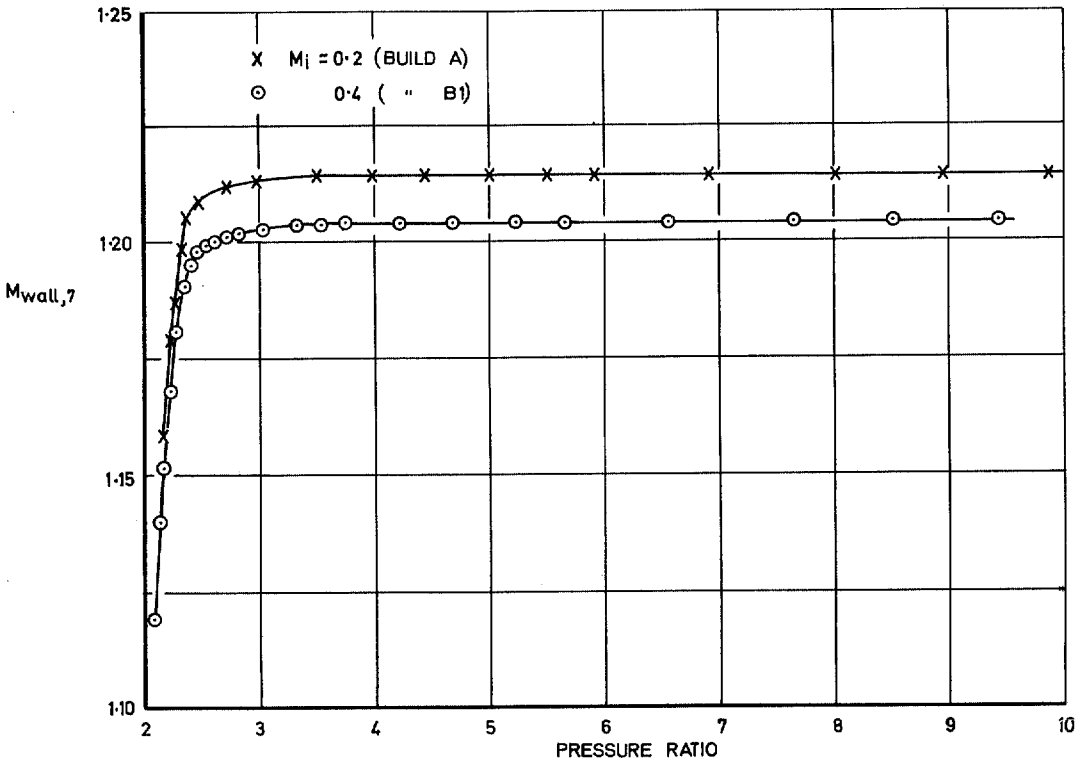

FIG. 7. Nozzle wall conditions near outlet.

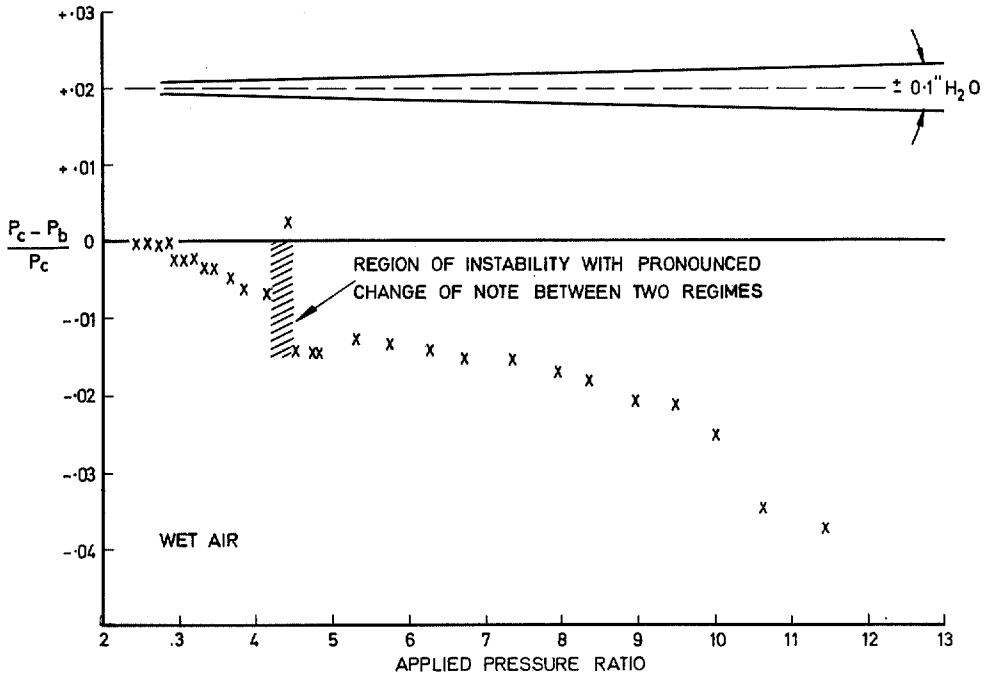

FIG. 8. Mean base pressure with $M_i \simeq 0{\cdot}2$ (Build A).

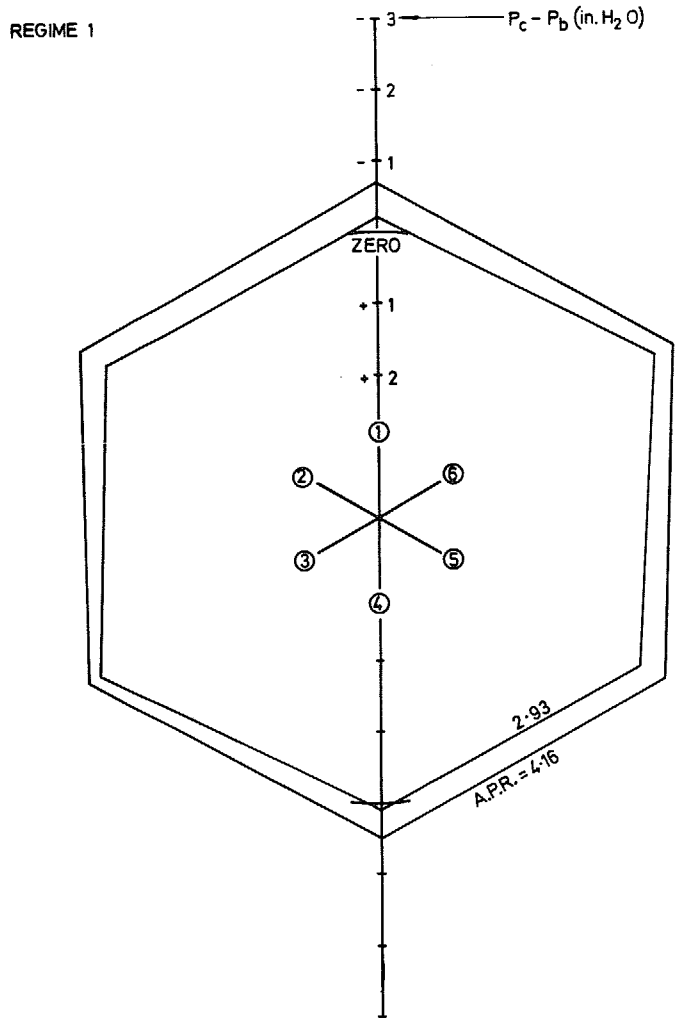

FIG. 9a. Circumferential variation of base pressure with $M_i \simeq 0{\cdot}2$ (Build A).

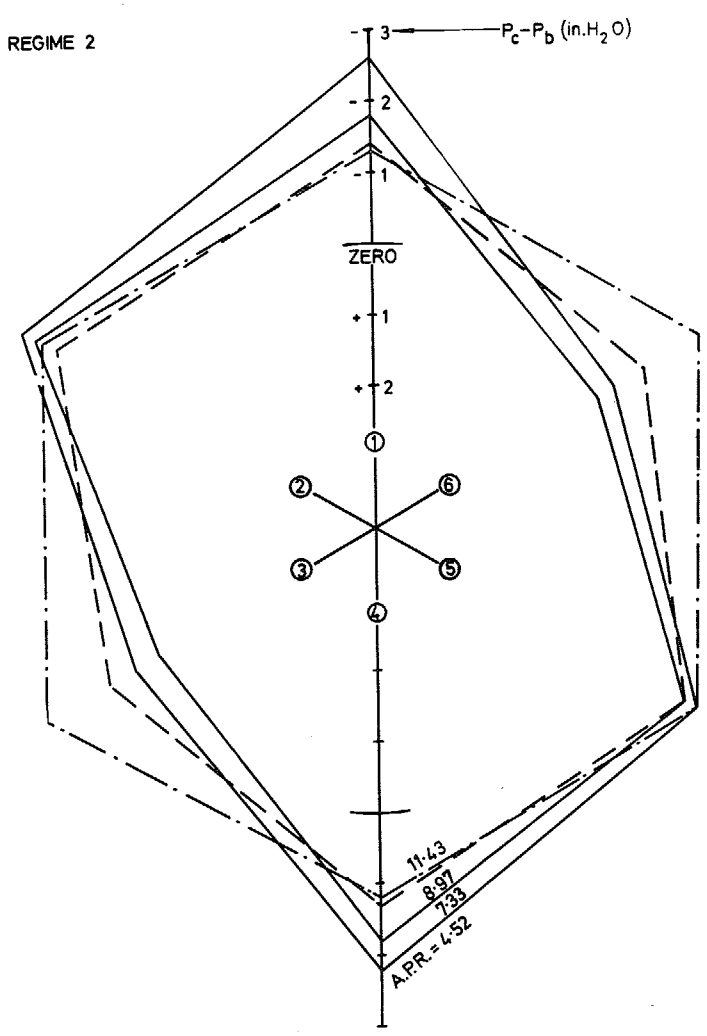

FIG. 9b. Circumferential variation of base pressure with $M_i \simeq 0{\cdot}2$ (Build A).

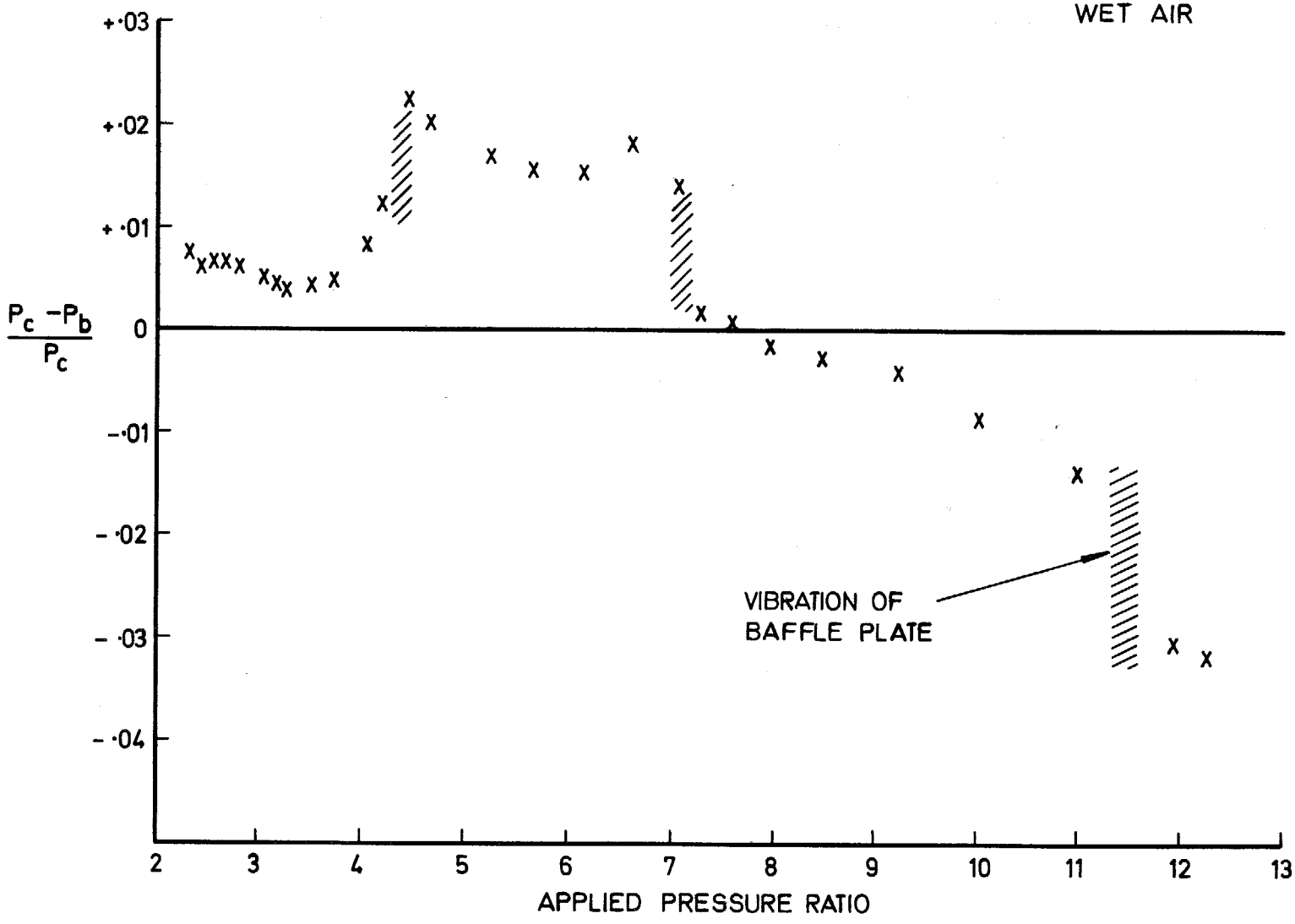

FIG. 10. Mean base pressure with $M_i \simeq 0{\cdot}4$ (Build B1).

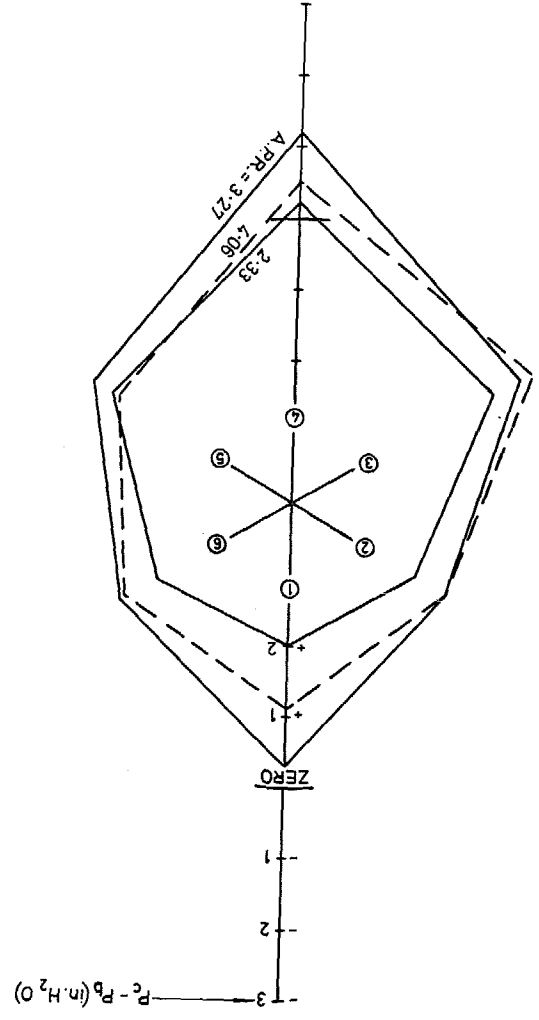

FIG. 11a. Circumferential variation of base pressure with $M_i \simeq 0{\cdot}4$ (Build B1).

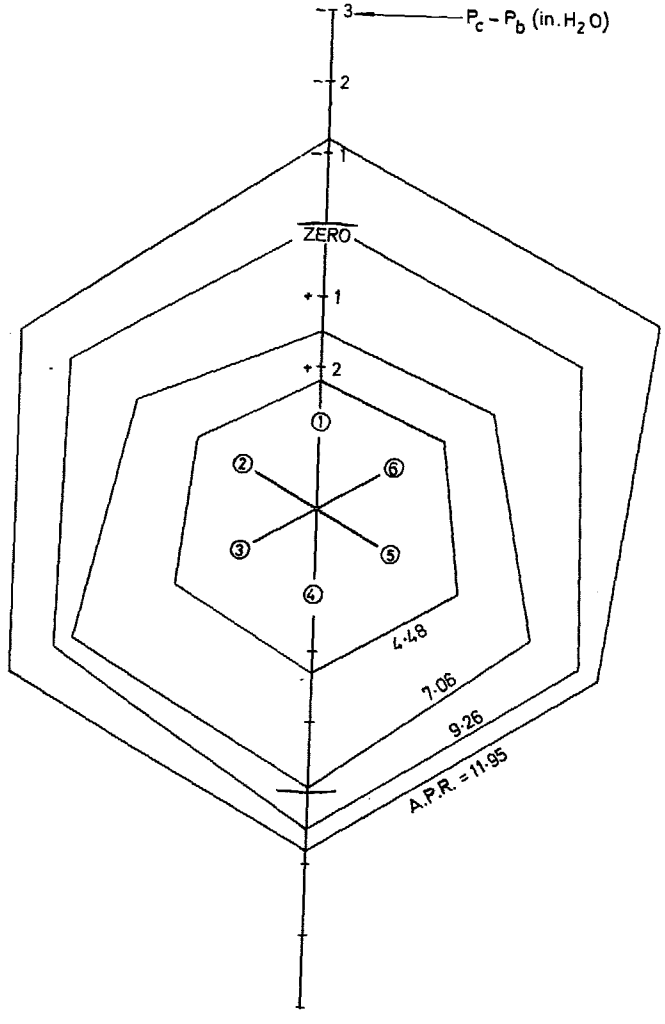

FIG. 11b. Circumferential variation of base pressure with $M_i \simeq 0{\cdot}4$ (Build B1).

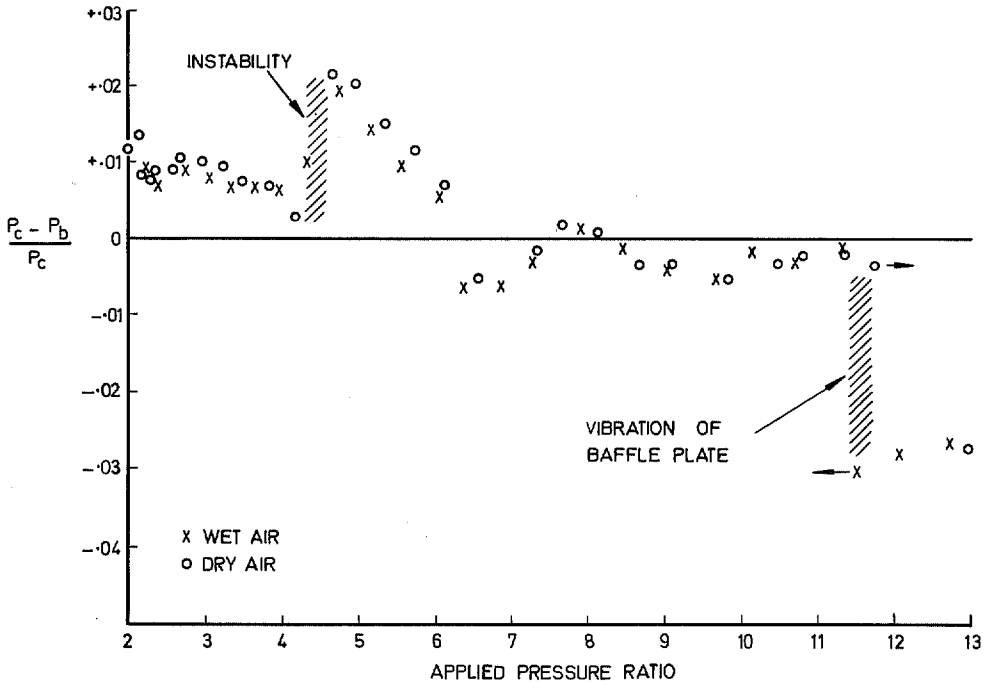

FIG. 12. Mean base pressure with $M_i \simeq 0{\cdot}4$ (Build B2 with baffle plate at outlet).

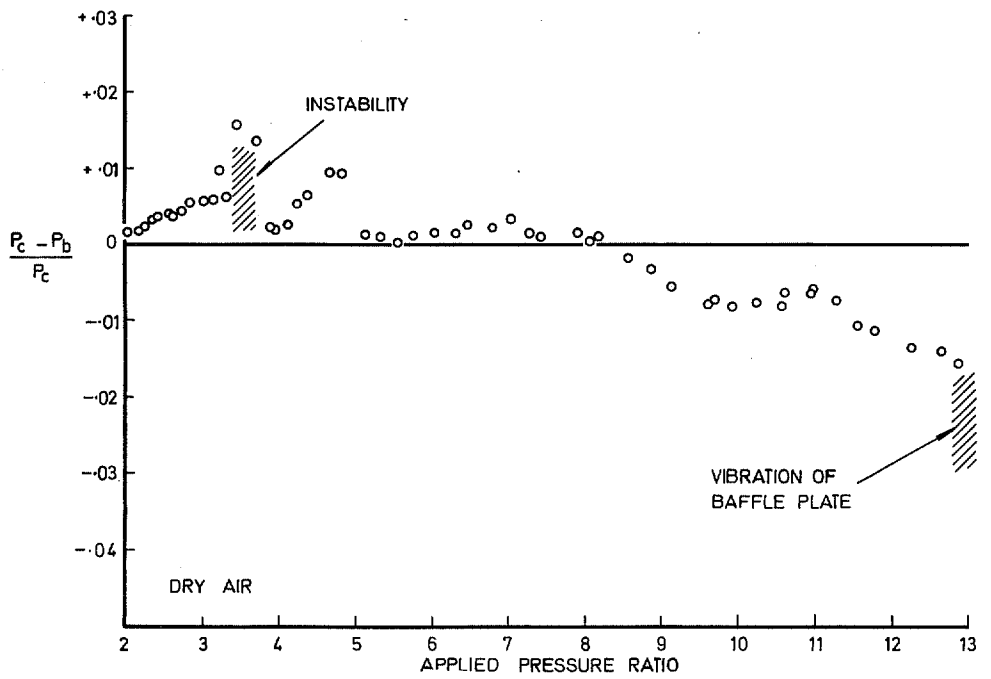

FIG. 13. Mean base pressure with $M_i \simeq 0{\cdot}4$ (Build B2 with baffle plate on parallel portion).

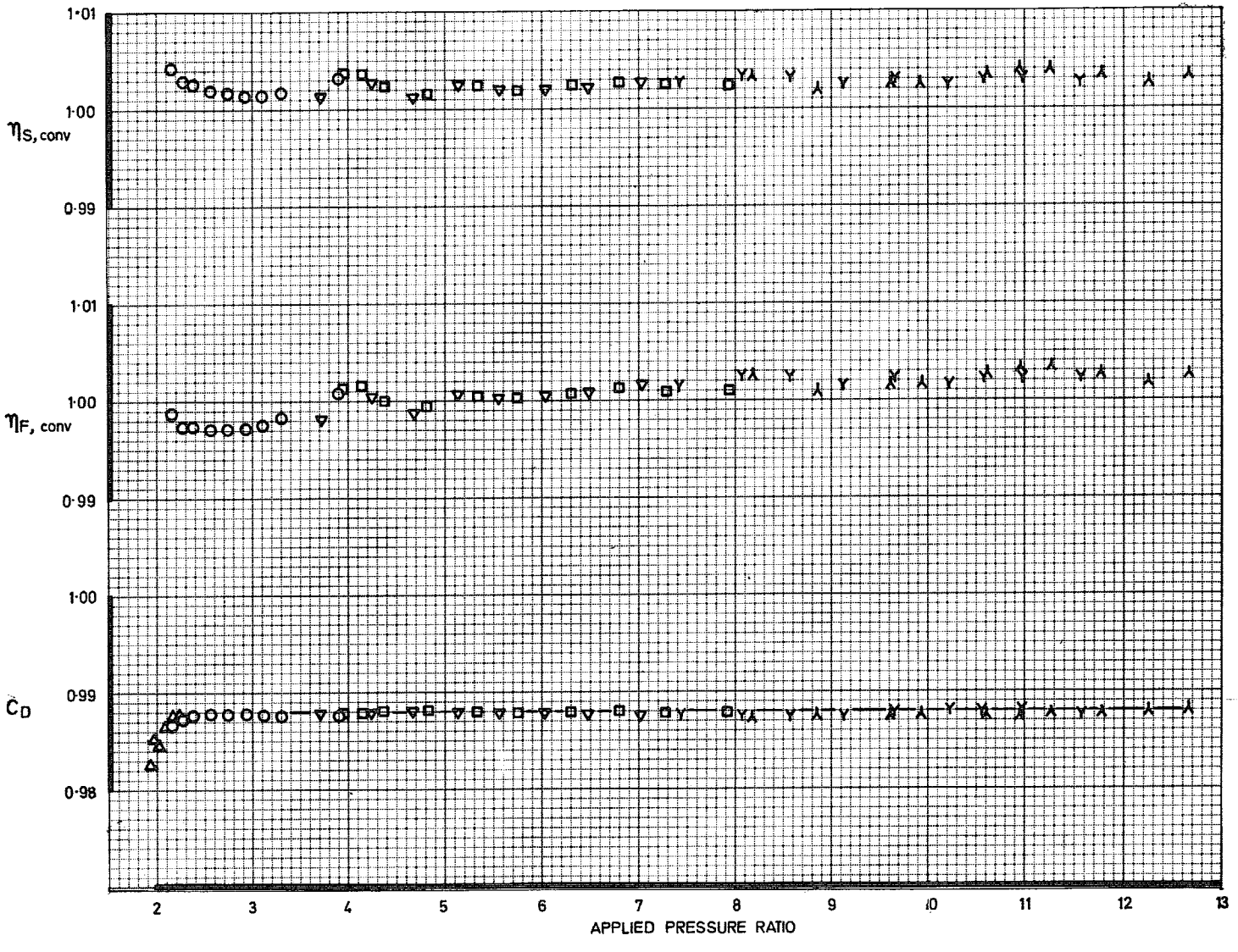

FIG. 14. Performance of nozzle with $M_i \simeq 0{\cdot}4$ (Build B2 with baffle plate on parallel portion).

Dd. 135646 K 5 Printed in Wales for Her Majesty's Stationery Office by Allens Printers (Wales) Limited

Published by
HER MAJESTY'S STATIONERY OFFICE

To be purchased from
49 High Holborn, London W.C.1
13A Castle Street, Edinburgh 2
109 St. Mary Street, Cardiff CF1 1JW
Brazennose Street, Manchester M60 8AS
50 Fairfax Street, Bristol BS1 3DE
258 Broad Street, Birmingham 1
7 Linenhall Street, Belfast BT2 8AY
or through any bookseller

R. & M. No. 3586

S.O. Code No. 23-3586